

# DIGITAL CLOSE-RANGE PHOTOGRAMMETRY USING ARTIFICIAL TARGETS

F.A. van den Heuvel, R.J.G.A. Kroon

Ingenieursbureau Geodelta, Oude Delft 175, 2611 HB DELFT, The Netherlands

R.S. Le Poole

Sterrewacht Leiden, P.O.Box 9513, 2300 RA LEIDEN, The Netherlands

## Abstract

A procedure for an automatic search and measurement of artificial targets in digital images for close-range photogrammetric applications is presented. Photographs taken with a semi metric 6x6 camera were digitized by the "ASTROSCAN" at the Sterrewacht Leiden. The especially designed targets contain a circular barcode for automatic identification. It is shown that this procedure improves both precision and productivity of the photogrammetric process.

**Key Words:** Close-range Photogrammetry, Image Matching, Image Quality, Scanner

## 1. Introduction

The objective of this study was the development of a fully automated procedure for close-range photogrammetry. An increase in productivity and improvement of precision will make photogrammetry even more attractive as a three-dimensional measuring technique.

The procedure developed by Ingenieursbureau Geodelta and Leiden Observatory (Sterrewacht Leiden) of the Leiden University consists of the following steps:

- digitalisation of photographs;
- digital search for the images of the targets;
- estimation of target positions in the images;
- reading the identification of the targets found;
- performing a bundle adjustment to arrive at three-dimensional target coordinates.

To test the procedure developed, a set of eight photographs was taken from a targeted indoor scene. A 6 x 6 cm semi-metric camera with black-and-white negative film was used. For comparison the photographs were measured in a conventional way as well, using a Kern DSR 11 analytical plotter. The bundle adjustment showed an improvement in precision of the result obtained by the automatic procedure relative to the precision obtained through the conventional photogrammetric procedure.

For the automation of the search, as well as for the identification of the targets found, the design of the targets plays an important role.

## 2. Target design

The targets were designed to facilitate automatic detection and identification. The target design consists of a white circle with a concentric ring on a black base. Around this there is another concentric ring in which a ten bit target identification is coded. The central circle is slightly oversized and has a small black dot in the middle to facilitate manual measurement. The rings are sized to allow for a realistic amount of defocus without losing the contrast to a significant extent. Sample targets are shown in figure 1.

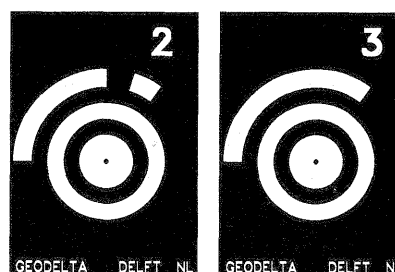


figure 1: two artificial targets

### 3. Digitalisation

Present technology allows computer access to the information content of photographs. To that end negatives must be digitized with sufficient accuracy, to avoid errors induced by the digitization process. For this reason we used the high precision scanner ASTROSCAN of Sterrewacht Leiden. The ASTROSCAN is a David Mann Monocomparator modified to allow computer controlled operation as a micro densitometer. A 128 element Reticon photodiode array is measuring the transmitted light from the photograph. Stepping motors control the positioning of this array in steps of 10  $\mu\text{m}$ . So pixels have a size of 10 x 10  $\mu\text{m}$  and a slightly bigger effective size of 13 x 13  $\mu\text{m}$ . Real-time application of a calibrated transformation of the transmission measured provides for photographic densities. From both the geometric and radiometric point of view the ASTROSCAN is a high precision scanner with a well documented performance.

**Geometry.** The repeatability of the pixel positioning of the ASTROSCAN is found to be 0.3  $\mu\text{m}$  RMS. This holds for the mean of a few hundred pixels. Local systematic deviations stay below 1  $\mu\text{m}$ . In figure 2 an error vectorfield of a repeatability test is plotted.

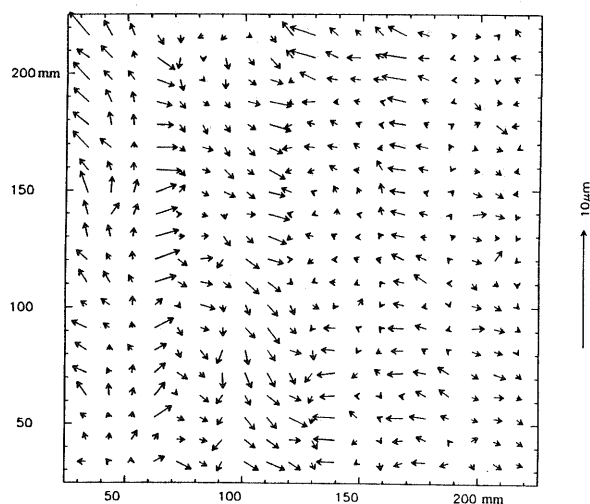


figure 2: error vectorfield of an Astroscan repeatability test

**Radiometry.** The measurement noise of the photodiodes being about 0.07% of full scale the noise in the densitometry is well below the photographic noise, except for very black pixels, where the transmitted light is less than about 0.5% of full scale. For such dark pixels a second effect distorting the radiometry comes into play: scattered

light in the optical system. For all less "overexposed" pixels the densitometric precision of the ASTROSCAN has been shown to be better than a few times 0.01%.

### 4. Search

For full automation of the procedure the targets present in the images have to be recognized automatically. The recognition results in approximate positions of the targets.

The algorithm used to detect the targets in the images was developed at Sterrewacht Leiden for the detection of astronomical objects in starplates. The first step in this procedure is the estimation of the background. In the astronomical applications the background consists of the pixels with the lowest densities. Objects consist of excess density in an area of the size of the Point Spread Function or slightly larger. The algorithm detects sets of adjacent pixels with a preset density difference above the background value.

This procedure applied in close-range photogrammetry will yield many more high density areas (supposedly "objects") than the ones that originate from the specially designed targets. In our experiment just over 5% of the objects found were part of a target image. All targets were detected.

To distinguish targets amongst all objects detected, a set of parameters is computed for every object. The parameters are used for a comparison with the characteristics of a target image.

The main characteristics used are the following:

- within limits set by the size of the target images two objects should be found at the same location (the images of the circle and the ring of the target);
- the size of these two objects should have a fixed ratio within bounds set empirically;
- the absolute size of the two objects should be within limits that depend on the scale of the photograph, which in turn is to be adapted to the physical size of the targets photographed.

For 9% of the targets only one object of the two was detected. Inconsistencies in excess of 35  $\mu\text{m}$  for the two supposedly identical positions is found in 17% of the cases, probably due to a large "curvature" in the estimated background and/or

illumination of the target at exposure. The regular difference in position in case of a double detection is about 15  $\mu\text{m}$ , which is an indication for the quality of these positions as start-estimates for the subsequent position estimation procedure.

Although it has not been tested, this astronomical target detection procedure is expected to give even better results if it is adapted for close-range photogrammetry. Especially the background estimation needs further investigation.

So far we only discussed the detection of targets. For the automatic position estimation of reseau crosses approximate locations are needed as well. With a sign reversal (densities lower than a chosen threshold below the "background" density) the procedure applied for target detection can be used for the reseau cross detection also. The main characteristics of reseaucrosses to be used for their recognition are:

- the known size (number of pixels) of a reseau cross image;
- the density of the reseau cross pixels should be among the lowest (and most likely a known fixed value) present in the image;
- the location of the reseaucrosses in a regular grid.

Although the procedure for searching reseaucrosses has not been implemented for this experiment, the detection of the reseaucrosses in the image is not expected to present any difficulty, apart for those in heavily underexposed areas.

In our experiment a wide range of photoscale and illumination of targets was used. Under regular circumstances and with a for close-range imagery optimized search method it will be possible to detect almost all complete target images. Images having defects f.i. due to partial obstruction will not only be difficult to detect, but usually it is very difficult to generalize algorithms to model their position estimation with sufficient success.

## 5. Measurement

The search method described in the previous paragraph can be seen as the first step in the position estimation process. The final improvement of the position estimate is made with the "least squares template matching" method. This matching

method requires startpositions with a precision of about 2 pixels (20  $\mu\text{m}$ ), in order to assure convergence of the iterative procedure. In those cases where the search method fails to produce a startposition with this precision, an intermediate step is necessary. In all three steps the procedures are different for reseaucrosses and targets.

### 5.1 Reseaucrosses

The startposition for a reseau cross is improved in a straight forward manner by detecting the four legs of the cross using a locally determined threshold density level. Then the positions of the pixels determined to belong to the cross legs are averaged using the measured densities for weighting. This yields a centre of gravity in density. The average of two opposite legs gives the improved position in one of the two directions. The procedure is coded with a (weak) constraint on the alignment of the cross legs and the scanning directions. The improved position has a precision better than 1 pixel (10  $\mu\text{m}$ ).

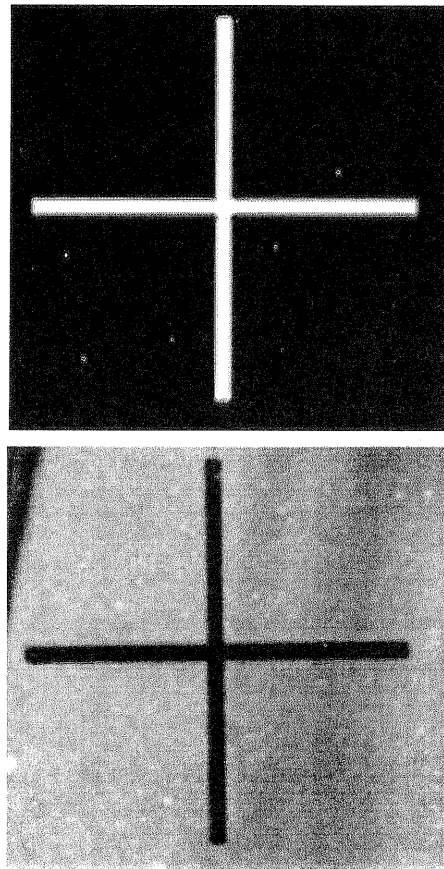


figure 3: template and reseau cross image (negative converted to positive)

For the final position estimation the least square template matching method was implemented. The template is a model of a reseau cross image. A binary image of an ideal reseau cross image (4 pixels wide and 100 pixels long) was generated and smoothed with a 2 x 2 averaging filter to approximate a convolution with the 20 μm wide Point Spread Function (P.S.F.) of regular photographic emulsions. The template and a sample reseau cross image is shown in figure 3. The matching of the template with the reseau cross image involves four parameters. The model can be written as follows:

$$g(x,y) = d_g * t(x-x_0, y-y_0) + g_0$$

with:

$g(x,y)$  = density at position  $x,y$  (the image)

$t(x,y)$  = template

$d_g$  = radiometric scale factor

$g_0$  = radiometric offset

$x_0,y_0$  = relative position template - image

The parameters can be split in two groups: the radiometric ( $d_g, g_0$ ) and the geometric parameters ( $x_0, y_0$ ). The addition of a geometric parameter for the rotation of the reseau cross relative to the coordinate system defined by the pixels has been tested. Although the estimated shift did not change significantly due to this model improvement (in the order of 0.1 μm), the estimated noise reduced by a factor 1.5. About the same reduction of the noise estimate was obtained by reducing the width of the cross-shaped matching window from 8 to 6 pixels. This is due to the reduction of the number of background pixels (see further on). The approximate position being known within the one pixel range, convergence did not pose any problem.

Although the density noise depends on the measured density itself (approximately linear for densities greater than 1), all pixels have been equally weighted. The estimated noise level should be interpreted as an average for the pixels within the matching window. The RMS-granularity of the emulsion used for the experiment is 1%. The effective pixelsize being 13 x 13 μm<sup>2</sup> the emulsion noise is about 3% for  $D(\text{ensity}) = 1$ . For an average density the emulsion noise level can be expected to be 4 - 5% for our pixelsize.

The reseau crosses with the lowest noise estimates were in the order of 6% of the average density level (5 parameter solution, matching window 6 pixels wide). This relatively high noise level originates mainly from the unmodelled non-uniform exposure of the reseau cross background. As mentioned before the width of the matching window has an influence on the noise estimate. This problem is inherent to the way in which the reseau crosses are projected on to the emulsion. Pre-illumination of the reseau grid can reduce, but not eliminate, the errors resulting from the non-uniformity of the background. Pre-illumination however solves the problems of lack of contrast between reseau crosses and background that occurs in cases of extreme under exposure of the background. However as the legs of the crosses are very narrow (about 40 μm = 2 P.S.F.) the bias that might result from an inadequate model for the background is assumed to be negligible. Only with a very steep mean gradient perpendicular to a leg might one expect a slight bias, which could hardly exceed 1 μm. So only the noise estimates are effected. As the precision of the position estimates for the crosses exceeds the quality of the description of film distortion by a large factor this presently is not relevant as the noise estimate cannot be exploited in a straightforward weighting scheme.

## 5.2 Targets

As for the reseau crosses, the startpositions for the targets should have a precision in the order of 2 pixels to guarantee convergence of the iterative parameter matching procedure. Although an optimized search procedure is expected to fulfil this requirement, an algorithm for startposition improvement has been implemented. This algorithm is based on the principle of autocorrelation and results in the symmetry point of the digital image. The idea is to find the symmetry point by finding the maximum correlation of the image with the image mirrored with respect to the (approximate) symmetry point. This is done through minimizing the two-dimensional function  $C(x_0, y_0)$ :

$$C(x_0, y_0) = \sum_x \sum_y (g(x, y) - g(2x_0 - x, 2y_0 - y))^2$$

with :

$C(x_0, y_0)$  = "correlation" function  
 $g(x, y)$  = density at x, y (the image)  
 $x_0, y_0$  = position of the symmetry point

Without interpolation, the correlation function can be evaluated on a grid with half pixel intervals. To obtain subpixel accuracy a 2-dimensional second order polynomial is fitted to a matrix of 3 by 3 datapoints of the correlation function. In this way the correlation function is approximated in an area the size of a pixel. The position of the minimum of the function gives the best estimate of the position of the symmetry point. The value of the minimum is an indication for the density noise in combination with the (lack of) symmetry present in the image.

To assure convergence of the matching procedure, apart from a relatively accurate position, the scale of the target should be approximated. In our experiment the scale of the targets could differ a factor 10 partly due to differences in photoscale, partly because of three different sizes of targets were used.

An indication for the scale is obtained through the autocorrelation procedure described above: the size of the so-called correlation window (circular area for which the autocorrelation function is evaluated) is chosen in such a way that a symmetry-criterion and a contrast-criterion is met. The measure for symmetry is defined by the minimum of the correlation function relative to the assumed emulsion noise. The contrast-criterion ensures a minimum size of the correlation window. Starting from a maximum size correlation window (depending on photoscale and size of the targets used) the size is decreased until both criteria are met. In this way the correlation window is fitted to the symmetric part of the target.

The standard deviation of the position using the autocorrelation method described above was estimated between 1% and 3% of a pixel for good quality images. The diameter of the correlation window generally was between 30 and 50 pixels. The estimated emulsion noise was between 2% and 4% of the average density. These estimates are optimistic because the correlation between neighbouring density measurements, due to pixel over-

lap (effective size at least 13 x 13  $\mu\text{m}$  depending on focus and only 10  $\mu\text{m}$  intervals), was neglected.

**Template matching.** Apart from the position of the target the scale is also provided with a first estimate. This facilitates convergence of the least squares template matching.

The template is an artificial digital image based on the target design. It contains only the circle and the ring of a target. The template image is smoothed with a 3 by 3 averaging filter to simulate convolution with the Point Spread Function. For target images the P.S.F. is wider than for reseau crosses (P.S.F. of the emulsion only) due to the influence of the lens system, atmosphere and defocussing. These effects differ between different targets. The same holds for the photoscale. The template is designed for the image of a slightly defocused target with average photoscale. The template and a sample image are shown in figure 4.



figure 4: template and target image

The eight parameter model for the least squares matching can be written as follows:

$$g(x,y) = d_g * t(A * (x-x_0, y-y_0)) + g_0$$

with:

$g(x,y)$  = density at  $x,y$  (the image)

$t(x,y)$  = template

$d_g, g_0$  = radiometric scale and offset

$A$  = affine transformation (2 x 2) matrix

$x_0, y_0$  = position of the template

An affine transformation is chosen to model the geometric transformation because this is a good local approximation of the projective transformation from object to photo. This holds for a target on a flat surface.

For the radiometric part of the model, as in the reseau cross matching a linear model is chosen.

For target images with a diameter of 40 pixels or more (circular matching window) the estimated precision of the position is around 1% of a pixel (0.1  $\mu$ m) standard deviation. This corresponds to a photoscale of about 1:100 for the large sized targets (40 mm diameter of the ring). For smaller target images the estimated standard deviation is in the order of 2% of a pixel. The formal variance drops linearly with an increase in diameter of the image size, because the number of gradient pixels increases linearly with the diameter. The estimated emulsion noise varies between 2.4% and 4.1% of the average density. Again correlation between density measurements have not been taken into account.

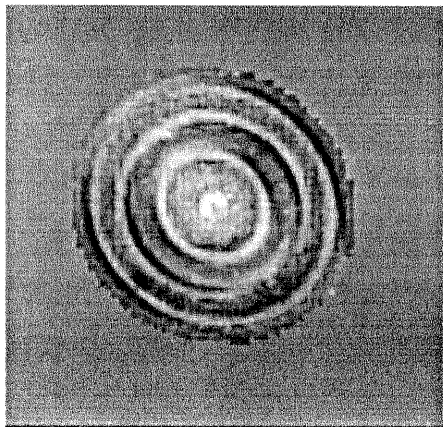


figure 5: sample residual image (enhanced radiometric scale)

In figure 5 a density residual image is depicted. The circular patterns show the imperfection of the

template model used.

In principle the result of the autocorrelation and the matching method can be expected to be the same. Comparison between the two is hindered by the difference in correlation/matching window size (and shape). However, the estimated positions correspond to the level of the estimated standard deviations, i.e. below 3% of a pixel difference for good quality images. The estimated density noise is somewhat higher than the known photographic noise for both methods, indicating model errors of rather the same size. Still the least squares matching method should be preferred for the final position estimation because it is more robust. The template makes the algorithm insensitive to mishaps in the images as long as they do not interfere with the target edges in the image. An other advantage of the least squares matching is the fact that the affine deformation of the target image is determined. This is needed for the automatic identification of the target.

## 6. Reading the target identification

To automate the identification of a target, each target has, next to its number printed in the upper right corner a circular binary code containing the same number. The binary code consists of 10 bits allowing for 1024 different numbers. If a part of the code is obscured, reading it is not possible. But if the code can be read in one of the images we have identified the target in the other images as well if the relative orientation of the images is known. The relative orientation of the images can be determined with a minimum set of targets identified.

Reading the circular binary code consists of 3 steps:

- sampling the code;
- determining the start point of the code;
- reading the code.

Using the previously solved affine deformation of the target image 200 samples of the binary code are taken from the image using bilinear interpolation for resampling. The sampling is done at regular angular distances, 10 samples per bit along the centre of the bar code ring. An example of a sampled code is depicted in figure 6. The location of the least significant bit is determined by

correlating the sampled code with a step function over half the circle. This is to detect the reference half of the circle. The other half of the circle contains the 10 bit code. Reading this code is done in a straight forward manner by comparing the densities in the bit centre with a threshold density level. This threshold depends on the densities found in the binary code.

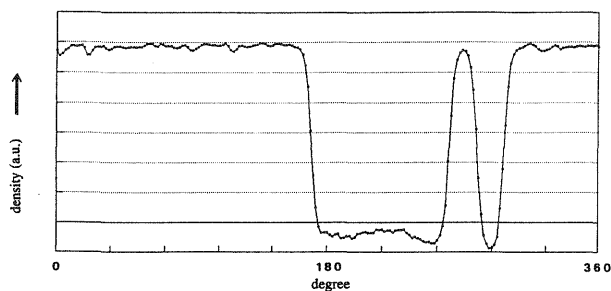


figure 6: sampled densities of binary coded identification

The experiment showed that if the least squares matching procedure was successful the binary code could be read also, except for those cases where a part of the code was occluded. Note that a significant improvement in Signal to Noise is still available by better modelling the image of the binary code. Obviously smaller photoscales are allowed before one runs into detection/recognition and estimation problems.

## 7. Bundle adjustment

The positions of targets and reseau crosses obtained through template matching are the basic input for the data reduction process to follow.

The data reduction consists of two steps:

- inner orientation;
- bundle adjustment.

In the inner orientation step the transformation of the measured positions of the targets to the system of the camera, represented by the imaged reseau crosses is performed.

In this step the film deformation is corrected for using the method of bilinear interpolation. The resulting positions of the target in the camera system are represented by their photocordinates.

The photocordinates of the targets and the approximate values of camera and target positions form the main input for the bundle adjustment step. The least squares bundle adjustment results in the 3-dimensional coordinates of the targets. The software package BINAER used for the bundle adjustment allows for simultaneous solution of camera parameters, a so-called "on-the-job" calibration of the camera.

In table 1 the results of the adjustments of the manual and the automatic measurements are generalized. Significantly more targets were measured manually than automatically. This is due to two effects: First a considerable number of targets were incomplete or deformed for testing purposes. Secondly, in contrast to the matching software, the operator can interpret the images that are incomplete and in this way he is able to measure most of the target images. The measurement of defected target images in combination with the resulting increase in redundancy leads to an increase of the estimated variance factor (table 1: all manual versus selection of manual observations). Comparing the adjustment of corresponding target measurements the digital approach shows a reduction in estimated variance by a factor 1.4 (table 1: select.manual - digital).

results BINAER	# targets	# target measurements	estimated standard deviat.	degrees of freedom
manual	104	599	4.1 $\mu\text{m}$	840
select. manual	72	227	3.5 $\mu\text{m}$	192
digital	72	227	3.0 $\mu\text{m}$	192

table 1: results of the bundle adjustment (8 photographs)

The gain in precision expected from the digital approach was less than anticipated. One error source was underestimated: the film deformation. Using bilinear interpolation correcting for film deformation errors up to 45  $\mu\text{m}$  leaves errors up to 2  $\mu\text{m}$ . Furthermore it became clear that next to improving measurement precision the model itself should be improved. For instance the lens and camera model should be refined. The automatically and manually measured photo coordinates match with a precision of 2  $\mu\text{m}$  RMS allowing an affine transformation between the two systems. Comparing this with the variance factors estimated in the bundle adjustment it can be concluded that

reduction of non-measurement error sources should be investigated.

## 8. Conclusions

This study shows that digital image processing can improve both the precision and the productivity of the close-range photogrammetry. In order to optimize these two aspects it is necessary to improve some parts of the digital photogrammetric process.

Looking at productivity the time needed for digitisation (6 hours per negative) should be reduced. A new version of the ASTROSCAN is being developed needing about half the time. If the need for faster digitalization arises using another digitizer should be considered. A CCD-camera is an alternative for obtaining the digital images. Then the problem of film deformation and therewith the need for reseaucrosses and their matching would be eliminated.

The computational burden of the matching process is a second productivity aspect. The 4 hours per negative needed in the experiment (for an average negative: 121 reseaucrosses and 50 targets) using a 80386 processor based PC. This can be reduced through optimization of the software and by utilizing a faster computer. However, these time aspects have only importance if results are needed within a short timescale. It should be noted that digitizer and computer can operate 24 hours a day without manual interaction.

As far as precision is concerned, the experiment showed an improvement of a factor 1.4 in variance. Further improvement is expected from a better film deformation model; also reduction of the film deformation itself should be aimed at. A second aspect influencing the precision is the camera model. Especially for a camera with a relatively short focal length (40 mm for the camera used in the experiment) an extension of the model with a few degrees of freedom is to be investigated.

## Literature

Ackermann F., 'Digitale Bildverarbeitung in der photogrammetrischen Stereo-auswertung' Stuttgart, Germany, 1989

Amdal K., Thune N., Dørum H., 'Correction of image deformations using B-spline surfaces in digital close-range photogrammetry' 'Close range Photogrammetry Meets Machine Vision' ISPRS Symposium proceedings Zürich, Switzerland, Sept.1990

Baarda W., 'Statistical Concepts in Geodesy' Neth. Geod. Comm., Publ. on Geodesy, New Series, Vol. 2, No. 4, Delft, The Netherlands, 1967

Bähr H.P., Vögtle T., 'Digitale Bildverarbeitung', Wichmann Verlag, Karlsruhe, Germany, 1991

Baltsavias E.P., Beyer H.A., Fritsch D., Lenz R.K., 'Fundamentals of Real-Time Photogrammetry' Tutorial Notes, Zürich, Switzerland, Sept. 1990

Buiten H.J., Clevers J.G.P.W. (ed.), 'Remote Sensing, theorie en toepassingen van landobservatie' Wageningen, The Netherlands, 1990

Förstner W., 'Prinzip und Leistungsfähigkeit der Korrelation und Zuordnung digitaler Bilder' Stuttgart, Germany, 1989

Fritsch D., 'Algorithms in Fast Vision Systems' Optical 3-D Measurement Technique, Gruen/Kahmen (ed.), pages 87-102, Germany, Sept.1989

Haarlem M.P. van, Katgert P., Tritton S., Le Poole R.S., 'The fidelity of photographic plate copies' Mon.Not.R.A.S., Leiden, The Netherlands 1991

Heuvel F.A. van den, 'Haalbaarheidsonderzoek digitale fotogrammetrie' Ing.bur. Geodelta BV, Rijswijk, The Netherlands, Jun. 1989